Differential Effects of Human Immunodeficiency Virus Type 1 Vpu on the Stability of BST-2/Tetherin[▽]

Amy J. Andrew, Eri Miyagi, and Klaus Strebel*

Laboratory of Molecular Microbiology, Viral Biochemistry Section, National Institute of Allergy and Infectious Diseases, NIH, Bethesda, Maryland 20892-0460

BST-2/CD317/tetherin is a host factor that inhibits the release of HIV-1 and other unrelated viruses. A current model proposes that BST-2 physically tethers virions to the surface of virus-producing cells. The HIV-1-encoded Vpu protein effectively antagonizes the activity of BST-2. How Vpu accomplishes this task remains unclear; however, it is known that Vpu has the ability to down-modulate BST-2 from the cell surface. Here we analyzed the effects of Vpu on BST-2 by performing a series of kinetic studies with HeLa, 293T, and CEMx174 cells. Our results indicate that the surface downregulation of BST-2 is not due to an accelerated internalization or reduced recycling of internalized BST-2 but instead is caused by interference with the resupply of newly synthesized BST-2 from within the cell. While our data confirm previous reports that the high-level expression of Vpu can cause the endoplasmic reticulum (ER)-associated degradation of BST-2, we found no evidence that Vpu targets endogenous BST-2 in the ER in the course of a viral infection. Instead, we found that Vpu acts in a post-ER compartment and increases the turnover of newly synthesized mature BST-2. Our observation that Vpu does not affect the recycling of BST-2 suggests that Vpu does not act directly at the cell surface but may interfere with the trafficking of newly synthesized BST-2 to the cell surface, resulting in the accelerated targeting of BST-2 to the lysosomal compartment for degradation.

HIV-1 must overcome several host defense mechanisms in order to establish an efficient infection. Trim-5α, APOBEC3G, and BST-2/tetherin are host restriction factors that target different stages of viral replication but are all regulated by type I interferons (4, 32, 39). BST-2 was originally identified as a membrane protein in terminally differentiated human B cells of patients with multiple myeloma (13, 35). BST-2 is a 30- to 36-kDa type II transmembrane protein consisting of 180 amino acids (19). The protein is predicted to have an N-terminal transmembrane domain and a C-terminal glycosylphosphatidylinositol (GPI) anchor (22). These two domains are separated by approximately 120 residues that constitute the protein's ectodomain and are predicted to form a 16- to 17-nm-long rod-like coiled-coil structure (18, 40, 45). The BST-2 ectodomain encodes three cysteine residues (3, 13, 35, 36), all of which can independently contribute to the formation of cysteine-linked dimers (3, 36), and is modified by N-linked glycosylation (3, 22, 35). The BST-2 protein associates with lipid rafts at the cell surface and on internal membranes, presumably the *trans*-Golgi network (9, 17, 22, 27).

BST-2 was previously identified as an interferon-inducible host factor responsible for the inhibition of HIV-1 virus release (33, 42). A current model suggests that BST-2 tethers mature virions to the cell surface by means of its N-terminal transmembrane domain and C-terminal GPI anchor (33). Indeed, immune electron microscopy confirmed that BST-2 could be found on virions tethered to the cell surface (10, 15, 16, 36). However, the distance between virions and the membrane determined by these techniques was often greater than 17 nm (10, 16, 36) and thus exceeded the maximum possible distance that can be bridged by BST-2 via a direct tethering mechanism.

BST-2 reduces the release of HIV-1. This function of BST-2 is antagonized by Vpu; however, the exact mechanism of how Vpu counteracts BST-2 is still unclear. Recent data suggest that the BST-2 transmembrane domain is crucial for interference by Vpu (7, 14, 28, 29, 36, 38). This is consistent with the previously reported critical importance of the Vpu transmembrane domain for the regulation of virus release (41). The interaction of Vpu and BST-2 results in the downregulation of BST-2 from the cell surface (15, 27, 29, 31, 37). The cellular site from which Vpu regulates BST-2 internalization has not been established. However, Vpu was previously found to colocalize with BST-2 in endosomes and the *trans*-Golgi network (7, 9, 17, 33, 37, 42).

Several studies reported the involvement of a proteasomal degradation pathway in the Vpu-induced down-modulation of BST-2 (7, 11, 26) and suggested a β-TrCP dependence (7, 26). Other studies proposed the involvement of a β-TrCP-dependent endolysosomal pathway (7, 20, 29). Irrespective of what mechanism is ultimately responsible for the reduction of BST-2 levels, the functional significance of the effect of Vpu on BST-2 stability remains unclear since Vpu can inhibit BST-2 function even in the absence of cell surface down-modulation or degradation (8, 12, 29, 30).

The current study aims at better defining the effects of Vpu on BST-2 through a variety of kinetic studies. Our results confirm previous reports that Vpu does not seem to affect the rate of internalization of surface-expressed BST-2 (8, 29). This suggests that the depletion of BST-2 from the cell surface by Vpu is due to interference with the resupply from within the cell. We also confirmed that Vpu can reduce the stability of

---

* Corresponding author. Mailing address: Viral Biochemistry Section, Laboratory of Molecular Microbiology, NIAID, NIH, Bldg. 4, Room 310, 4 Center Drive, MSC 0460, Bethesda, MD 20892-0460. Phone: (301) 496-3132. Fax: (301) 402-0226. E-mail: kstrebel@nih.gov.

newly synthesized BST-2 in transfected 293T cells via an endoplasmic reticulum (ER)-associated degradation pathway, as reported previously (11). However, this effect was dependent on the high-level expression of Vpu. Surprisingly, virus-encoded Vpu neither affected the stability of newly synthesized BST-2 in transiently transfected 293T cells nor altered the stability of newly synthesized endogenous BST-2 in virus-infected HeLa or CEMx174 cells. Instead, virus-expressed Vpu acted at a post-ER level to increase the turnover of mature BST-2. Our results indicate that Vpu interferes with the trafficking of BST-2 to the cell surface from a post-ER compartment, presumably by rerouting BST-2 to the lysosomal compartment for degradation.

MATERIALS AND METHODS

Plasmids. The full-length infectious HIV-1 molecular clone pNL4-3 and the Vpu deletion mutant pNL4-3/Udel were described previously (1, 21). For the transient expression of Vpu, the codon-optimized vector pcDNA-Vphu was employed (34). Plasmid pcDNA-BST-2 encodes untagged human BST-2 and was constructed as described previously (3). For the expression of green fluorescent protein (GFP), the pEGFP-N1 vector (Clontech, Mountain View, CA) was used.

Antisera. Polyclonal anti-BST-2 antiserum directed against the extracellular portion of BST-2 was described previously (3, 30) and is freely available through the NIH AIDS Research and Reference Reagent Program (catalog number 11721; https://www.aidsreagent.org). A p24 antibody (KC57-RD1; Coulter Corp., Hialeah, FL) was used for fluorescence-activated cell sorter (FACS) analysis to determine the efficiency of infection. Polyclonal anti-Vpu serum (rabbit) directed against the cytoplasmic domain of Vpu expressed in *Escherichia coli* was used for the detection of Vpu. This antibody is freely available through the NIH AIDS Research and Reference Reagent Program (catalog number 969; https://www.aidsreagent.org). Tubulin was identified by using monoclonal antibodies (Sigma-Aldrich, Inc., St. Louis, MO).

Tissue culture and transfections. HeLa and 293T cells were propagated in Dulbecco's modified Eagle's medium (DMEM) containing 10% fetal bovine serum (FBS). CEMx174 cells were maintained in RPMI 1640 medium containing 10% FBS. For transfection, cells were grown in 25-cm^2 flasks to about 80% confluence. Cells were transfected by using TransIT-LT1 (Mirus, Madison, WI) or LipofectAMINE Plus (Invitrogen Corp., Carlsbad, CA) according to the manufacturers' recommendations. The total amount of transfected DNA was 5 μg and was kept constant in all samples of any given experiment by adding empty vector DNA as appropriate. Cells were harvested at 24 h posttransfection.

Virus preparation. Virus stocks for infection were prepared by transfecting 293T cells with appropriate plasmid DNAs. Virus stocks pseudotyped with the vesicular stomatitis virus G glycoprotein (VSV-G) were prepared by cotransfecting 0.5 μg of pCMV-VSVg along with 4.5 μg of the viral vector. Virus-containing supernatants were harvested 48 h after transfection. Cellular debris was removed by centrifugation (3 min at 3,000 × g), and clarified supernatants were filtered (0.45 μm) to remove residual cellular contaminants. Virus stocks were stored at −80°C.

FACS analysis. Cells were washed twice with ice-cold 20 mM EDTA–phosphate-buffered saline (PBS) and incubated for 15 min at 4°C for the detachment of cells, followed by 2 washes in ice-cold 1% bovine serum albumin (BSA)–PBS. Cells were treated for 10 min with 50 μg of mouse IgG (Millipore, Temecula, CA) to block nonspecific binding sites. Cells were incubated with primary antibody (anti-BST-2) for 30 min at 4°C. Cells were then washed twice with ice-cold 1% BSA–PBS, followed by the addition of allophycocyanin (APC)-conjugated anti-rabbit IgG secondary antibody (Jackson Immuno Research Lab Inc., West Grove, PA) in 1% BSA–PBS. Incubation was done for 30 min at 4°C in the dark. Cells were then washed twice with ice-cold 1% BSA–PBS and fixed with 1% paraformaldehyde in PBS. Finally, cells were analyzed with a FACSCalibur instrument (BD Biosciences Immunocytometry Systems, Mountain View, CA). For determining the percentage of infected HeLa cells, cells were permeabilized and stained with p24 antibody. Data analysis was performed by using Flow Jo software (Tree Star, San Carlos, CA). For the gating of transfected cells, pEGFP-N1 (Clontech, Mountain View, CA) was cotransfected. For measuring the rate of endocytosis, cells were suspended in DMEM and incubated at 37°C for the indicated times after primary staining and washing. After incubation, cells were washed twice with ice-cold 1% BSA–PBS and stained with APC-conjugated anti-rabbit IgG secondary antibody.

Metabolic labeling and immunoprecipitations. Infected or transfected cells were washed with PBS, scraped (HeLa and 293T cells), and suspended in 3 ml labeling medium lacking methionine and cysteine (MP Biomedicals, Solon, OH). Cells were incubated for 15 min at 37°C to deplete the endogenous methionine and cysteine pool. Cells were then pelleted, suspended in 600 μl of labeling medium containing 350 μCi of Expres^{35}S^{35}S protein labeling mix (Perkin-Elmer, Shelton, CT), and pulse-labeled at 37°C for the times indicated in the text. Cells were pelleted and suspended in complete RPMI medium, and equal volumes were aliquoted into separate tubes (1 tube per time point) containing 1 ml each of prewarmed complete RPMI medium. After the indicated chase times, cells were pelleted and frozen on dry ice. Cells were lysed in 200 μl of lysis buffer (10 mM Tris [pH 7.2], 140 mM NaCl, 8 mM Na$_2$HPO$_4$, 2 mM NaH$_2$PO$_4$, 1% Igepal CA-630, 0.5% sodium dodecyl sulfate, 1.2 mM deoxycholic acid) and incubated on ice for 5 min. Cell lysates were pelleted at 13,000 × g for 2 min to remove insoluble material. The supernatants were precleared by incubation with protein A-Sepharose for 1 h. Precleared lysates were incubated with BST-2 antibody for 2 h at 4°C, followed by the addition of protein A-Sepharose. Beads were washed twice with wash buffer (50 mM Tris [pH 7.4], 300 mM NaCl, 0.1% Triton X-100). Bound proteins were eluted by heating in sample buffer for 10 min at 95°C, separated by SDS-PAGE, and visualized by fluorography. All immunoprecipitations were done three times. Quantitations were done by PhosphorImager analysis of the radioactive gels.

Immunoblotting. For immunoblot analyses of intracellular proteins, whole-cell lysates were prepared as follows. Cells were washed once with PBS, suspended in PBS (400 μl per 10^7 cells), and mixed with an equal volume of sample buffer (4% SDS, 125 mM Tris HCl [pH 6.8], 10% 2-mercaptoethanol, 10% glycerol, and 0.002% bromophenol blue). Proteins were solubilized by boiling for 10 to 15 min at 95°C. Residual insoluble martial was removed by centrifugation (2 min at 15,000 rpm in an Eppendorf Minifuge). Cell lysates were subjected to SDS-PAGE; proteins were transferred onto polyvinylidene difluoride (PVDF) membranes and reacted with appropriate antibodies as described in the text. Membranes were then incubated with horseradish peroxidase-conjugated secondary antibodies (Amersham Biosciences) and visualized by enhanced chemiluminescence (ECL; Amersham Biosciences, Piscataway, NJ).

RESULTS

Vpu does not increase the rate of BST-2 internalization. The expression of BST-2 on the cell surface interferes with the release of virus particles in a mechanism that is not yet completely understood (for a review, see reference 2). The presence of Vpu in BST-2-positive HeLa cells is associated with a reduction of BST-2 surface levels, as exemplified in Fig. 1A. BST-2 is an integral membrane protein that is synthesized at the ER membrane. From there, the protein is transported to the cell surface. Like every cell surface marker, BST-2 is eventually internalized. Constant surface BST-2 levels are maintained presumably through the recycling of internalized protein as well as a resupply of *de novo*-synthesized protein from the ER. Thus, the Vpu-induced cell surface down-modulation of BST-2 can be accomplished in three possible ways: (i) a more rapid internalization of cell surface BST-2, (ii) a reduced rate of recycling of internalized BST-2 back to the cell surface, or (iii) a reduced resupply of *de novo*-synthesized BST-2 from within the cell.

To discriminate between these possibilities, we first measured the rates of BST-2 internalization in the presence or absence of Vpu. BST-2 expressed at the surface of HeLa cells was incubated with BST-2-specific antibody at 4°C to block internalization. Excess antibody was washed off, and the fate of BST-2–antibody complexes was monitored subsequent to shifting the temperature back to 37°C. BST-2–antibody complexes remaining at the cell surface were measured by FACS analysis at various times after the temperature shift (Fig. 1B). We found that about 10 to 20% of surface BST-2 was internalized within 2 min. A subsequent further reduction in surface BST-2
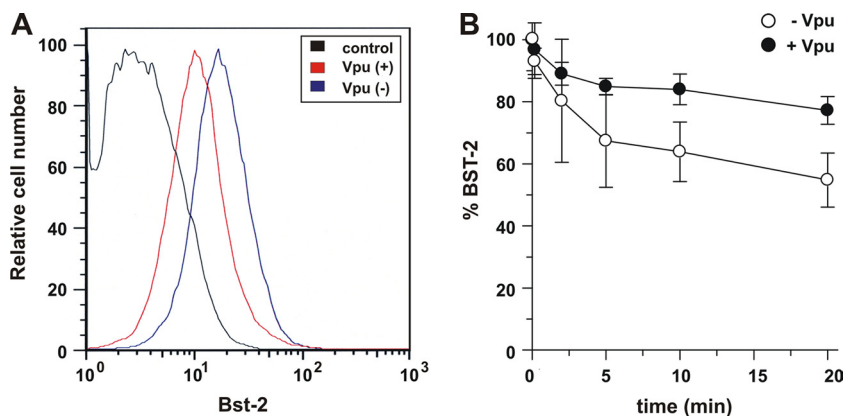
FIG. 1. Vpu reduces BST-2 levels independently of the rate of endocytosis of BST-2. (A) HeLa cells were transfected with 1 μg of pEGFP-N1 with [Vpu(+)] or without [Vpu(−)] 1 μg of pcDNA-Vphu. The total DNA was adjusted to 5 μg with empty vector DNA. Cells were stained with BST-2 antibodies and analyzed with a FACSCalibur instrument. Samples were gated for GFP expression, which was used as a marker for transfected cells. As a control, HeLa cells were stained with preimmune serum (control). (B) Cells were transfected as described above for A, harvested 24 h after transfection, labeled at 4°C with antibody to BST-2, and then incubated at 37°C for the indicated times. Cells were then stained with a secondary antibody and analyzed with a FACSCalibur instrument. Samples were gated for GFP-positive cells. The mean fluorescence intensity of the time zero cells for each population was defined as 100% BST-2 surface expression. Plotted data were derived from five independent experiments. Error bars represent standard errors of the means.

occurred at a lower rate and reached 60 to 80% of the initial BST-2 level after 20 min. An extension of the internalization assay to 60 min did not reveal any further reduction in BST-2 antibody detection at the cell surface, suggesting that a steady-state plateau was reached after about 20 min (data not shown). Importantly, the presence of Vpu did not enhance the rate of BST-2 internalization (Fig. 1B, closed circles). In fact, we observed a lower rate of BST-2 endocytosis in the presence of Vpu. These results are consistent with recent data from other laboratories (8, 29) suggesting that Vpu does not downregulate cell surface BST-2 through accelerated endocytosis. The fact that not all of the surface-labeled BST-2 was internalized but reached a plateau at about 60 to 80% of the initial level suggests that BST-2 rapidly cycles back to the cell surface and establishes an equilibrium within 10 to 20 min. Intriguingly, Vpu did not reduce the steady-state equilibrium of cell surface BST-2. If anything, steady-state levels of surface BST-2 were higher in the presence of Vpu than in its absence (Fig. 1B). The apparent dichotomy of these results with the data shown in Fig. 1A, demonstrating a net loss of surface BST-2 in the presence of Vpu, can be explained if one assumes that Vpu does not inhibit the recycling of internalized BST-2 back to the cell surface but controls the trafficking of newly synthesized BST-2 to the cell surface to supplement BST-2 that has been lost through its natural turnover.

Vpu affects the stability of mature BST-2 in HeLa cells. Since Vpu does not accelerate the rate of BST-2 endocytosis and does not appear to affect the recycling of BST-2 to the cell surface, we focused on our third model, which is that Vpu reduces the trafficking of de novo-synthesized BST-2 to the cell surface. Therefore, we next studied the possible effect of Vpu on BST-2 stability. Vpu is known to induce the ER-associated degradation of CD4 (6, 25, 43). It is therefore conceivable that Vpu similarly targets BST-2 in the ER by directing it into a degradative pathway. Indeed, we and others previously reported that the expression of Vpu can result in reduced steady-

state levels of BST-2 in HeLa or 293T cells, especially when Vpu is expressed at high levels (3, 5, 7, 11, 17, 20, 23, 26, 30).

Newly synthesized BST-2 is modified in the endoplasmic reticulum (ER) by the attachment of high-mannose carbohydrates (3, 22, 35). This is exemplified in Fig. 2A, where BST-2 was expressed in transiently transfected 293T cells. Pulse-labeling for 30 min revealed discrete protein bands of approximately 29 kDa (Fig. 2A, lane 2). We refer to this form of BST-2 as "immature BST-2," since it represents a protein with high-mannose-type carbohydrate modifications (3). As BST-2 exits the ER and traffics through the Golgi/trans-Golgi network, the carbohydrate moieties are further modified by the addition of complex carbohydrates (3). These modifications are not uniform and result in a diffuse smear with an apparent molecular mass of ~30 to 40 kDa (Fig. 2A, lane 3). We refer to this form of BST-2 as "mature BST-2." Mature BST-2 becomes apparent following a 30-min chase of metabolically labeled protein (Fig. 2A, lane 3). Two additional proteins of about 45 to 50 kDa are also apparent after the immunoprecipitation of metabolically labeled samples with the BST-2-specific antibody (marked by asterisks in Fig. 2A). The same two proteins are also immunoprecipitated from untransfected 293T cells (Fig. 2A, lane 1), suggesting that they are unrelated to BST-2 and represent nonspecific background. These nonspecific bands are also apparent in immunoprecipitations of metabolically labeled HeLa cells (e.g., see Fig. 2B) and CEMx174 cells (Fig. 3B) and were used as a guide for locating mature BST-2 on the gels.

To gauge Vpu's effect on BST-2 stability in the course of a virus infection, we prepared stocks of wild-type (wt) and Vpu-deficient NL4-3 virus in 293T cells. Viruses were pseudotyped with VSV-G for an expanded host range as well as to increase the viral titer. HeLa cells were infected with the pseudotyped virus stocks at a multiplicity of infection (MOI) of approximately 1. Under those conditions up to 75% of the cells produced viral Gag proteins, as determined by FACS analysis (data not shown). Twenty-four hours after infection, cells were
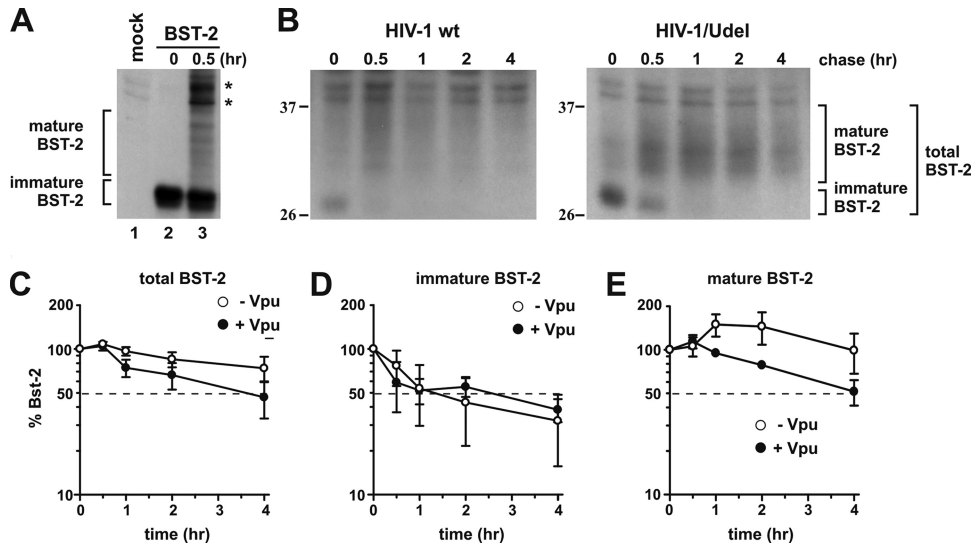
FIG. 2. Vpu accelerates the turnover of mature endogenous BST-2 in HeLa cells. (A) 293T cells were transfected with 1 μg of Bst-2, pulse-labeled for 30 min by the addition of ³⁵S-labeled amino acids, and chased for 30 min in complete medium. Mock represents untransfected cells labeled and immunoprecipitated in a similar manner. (B) HeLa cells were infected with pCMV-VSVg-pseudotyped pNL4-3 or pNL4-3/Udel virus along with 8 μg/μl polybrene. Twenty-four hours after infection cells were pulse-labeled for 1 h at 37°C by addition of ³⁵S-labeled amino acids and chased for the indicated time intervals in complete medium. BST-2 was immunoprecipated with specific antibodies. A representative result is shown. The position of molecular weight standards is shown on the left. (C) The percentage of BST-2 remaining at each time point was calculated relative to the signal at time zero. (D and E) Total levels of BST-2 were calculated by adding both immature BST-2 (D) and mature BST-2 (E). Mature BST-2 and immature BST-2 are indicated on the right. Plotted data are derived from three independent experiments. Error bars represent standard errors of the means.

metabolically labeled for 60 min and chased for up to 4 h as described in Materials and Methods. Initial attempts to shorten the labeling time to 30 min as was done for Fig. 2A failed, presumably due to the low rate of BST-2 synthesis in

these cells (data not shown). Lysates from samples collected at individual time points were immunoprecipitated with BST-2-specific antibody. The immunoprecipitated products were analyzed by SDS-PAGE followed by fluorography (Fig. 2B).
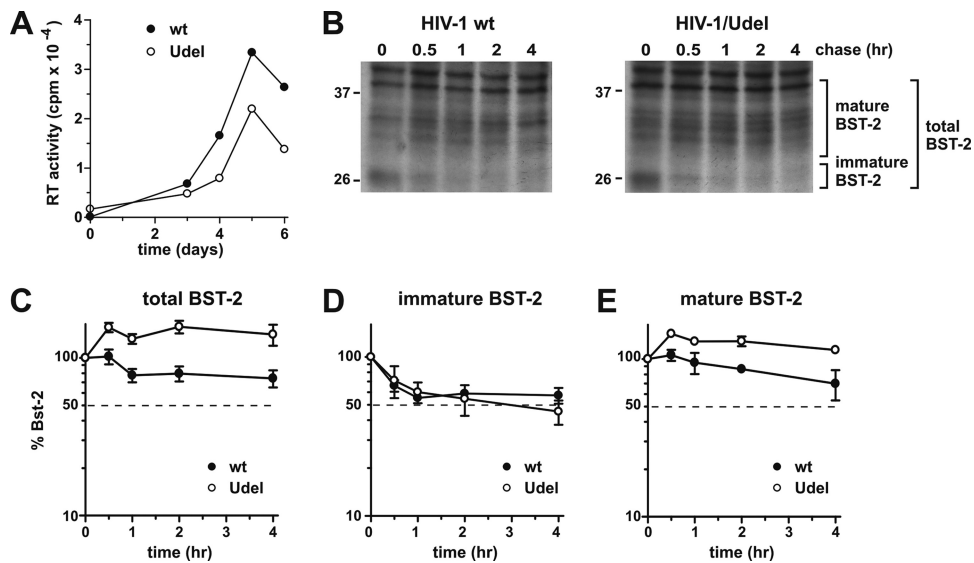

FIG. 3. Vpu accelerates the turnover of mature endogenous BST-2 in CEMx174 cells. (A) CEMx174 cells were infected with equal reverse transcriptase (RT) units of wt NL4-3 and NL4-3/Udel virus stocks produced in 293T cells. Virus replication was monitored by measuring the virus-associated reverse transcriptase activity in culture supernatants as described previously (44). (B) On day 5 after infection cells were pulse-labeled for 1 h at 37°C by the addition of ³⁵S-labeled amino acids and chased for the indicated time intervals in complete medium. BST-2 was immunoprecipitated with specific antibodies. A representative experiment is shown. Mature BST-2 and high-mannose BST-2 are indicated. The position of molecular weight standards is shown on the left. (C) The percentage of BST-2 remaining at each time point was calculated relative to the signal at time zero. (D and E) Total levels of BST-2 were calculated by adding both immature BST-2 (D) and mature BST-2 (E). Plotted data are derived from three independent experiments. Error bars represent standard errors of the means.

BST-2-specific bands were quantified by PhosphorImager analysis, and results were plotted as a function of time (Fig. 2C to E). Analysis of the total (i.e., immature plus mature) BST-2 protein revealed a more rapid decay of BST-2 in the presence of Vpu (Fig. 2C, solid circles) than in cells infected with a Vpu-deficient virus (Fig. 2C, open circles). To see if the increased decay of total BST-2 by Vpu was due to the accelerated degradation of newly synthesized immature BST-2 in the ER, we separately quantified the immature high-mannose form of BST-2, representing the ER-associated fraction of BST-2 (Fig. 2D), and the 30- to 40-kDa form of BST-2 carrying complex carbohydrate modifications, representing mature BST-2 that has exited the ER (Fig. 2E). We noticed an initial increase in the signal intensities of total and mature BST-2 at the early-chase time points, followed by a gradual decline (Fig. 2C and E). This is presumably due to a change in the affinity of our antibody as the BST-2 protein matures.

The level of total BST-2 in the presence of Vpu was reduced about 45% after 4 h of chase (Fig. 2C, solid circles), while in the absence of Vpu, total BST-2 levels remained at ~80% of the initial level (Fig. 2C, open circles). Surprisingly, Vpu had no discernible effect on immature BST-2, which rapidly declined at very similar rates in the presence or absence of Vpu (Fig. 2D). In contrast, Vpu accelerated the turnover of mature BST-2 (Fig. 2E). The half-life of mature BST-2 in the presence of Vpu was about 4 h (Fig. 2E, solid circles), while, based on the slope of the graph, the half-life of mature BST-2 was projected to be about 8 h in the absence of Vpu (Fig. 2E, open circles). We conclude that Vpu does not cause an ER-associated degradation of newly synthesized endogenous BST-2 but instead accelerates the turnover of mature BST-2 from a post-ER compartment.

The effect of Vpu on the stability of endogenous BST-2 is not cell type specific. We next wanted to ensure that the effects of Vpu on BST-2 are not limited to HeLa cells. We had previously analyzed a variety of cell lines susceptible to spreading HIV infection and found that CEMx174 cells express high levels of BST-2 and that virus release from these cells was Vpu dependent (30). To determine the stability of BST-2 following infection by HIV-1, CEMx174 cells were infected with wild-type and Vpu-deficient virus stocks produced in 293T cells in the absence of VSV-G. Infection was monitored by measuring virus-associated reverse transcriptase activity in the culture supernatants at various times after infection (Fig. 3A). Virus replication for both wild-type and Vpu-deficient viruses peaked on day 5 in this experiment (Fig. 3A). On day 5 we performed a pulse-chase analysis of BST-2 as described in the legend of Fig. 2 (Fig. 3B). As with HeLa cells, total levels of BST-2 in the absence of Vpu remained stable over the duration of the experiment (Fig. 3C, open circles). The presence of Vpu induced a reduction of total BST-2 levels to ~70% of the starting level, which is comparable to the Vpu-induced reduction observed with HeLa cells (Fig. 2C). Importantly, however, as in HeLa cells, Vpu did not increase the turnover of immature BST-2 in CEMx174 cells (Fig. 3D). Instead, Vpu affected the accumulation of mature BST-2 in CEMx174 cells (Fig. 3E). From these experiments we conclude that the effect of Vpu on the stability of mature BST-2 as well as the lack of an effect on immature BST-2 are not HeLa cell specific.
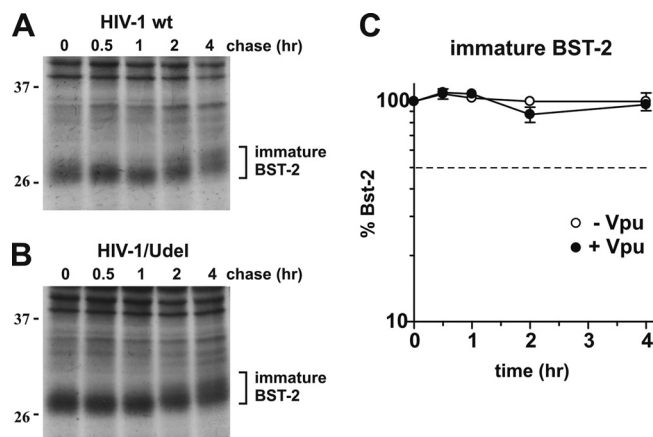

FIG. 4. (A and B) CEMx174 cells were infected with equal reverse transcriptase units of wt NL4-3 (A) and NL4-3/Udel (B) virus stocks produced in 293T cells as described in the legend of Fig. 3. On day 5 after infection cells were pulse-labeled as described in the legend of Fig. 3, with the addition of BfA during the pulse and chase at 5 μg/ml. A representative result is shown. The position of molecular weight standards is shown on the left. (C) Graph comparing the levels of the immature form of BST-2 from cells infected by wt HIV-1 (closed circles) and HIV-1/Udel (open circles). Plotted data are derived from three independent experiments. Error bars represent standard errors of the means.

Vpu fails to induce ER-associated degradation of endogenous BST-2 in CEMx174 cells. To further demonstrate that the disappearance of immature BST-2 in HIV-infected CEMx174 cells is not due to degradation in the ER but results from the subsequent complex carbohydrate modification of the protein, we repeated the pulse-chase analysis of CEMx174 cells as shown in Fig. 3, except for the presence of brefeldin A (BfA). BfA is a fungal metabolite that blocks the export of newly synthesized membrane proteins from the ER (24). We had previously employed BfA in our characterization of the Vpu-mediated degradation of CD4 and found that the retention of CD4 in the ER by BfA treatment greatly accelerated the degradation of CD4 (43). Interestingly, the effect of BfA on the half-life of BST-2 was quite the opposite: the presence of BfA stabilized the immature form of BST-2 during the pulse-chase analysis irrespective of whether the cells were infected by wild-type or Vpu-deficient HIV-1 (Fig. 4A and B). The quantitation of immature BST-2 from Fig. 4A and B revealed that in the presence of BfA, only 10% of the labeled protein was lost during the 4-h observation period (Fig. 4C). Extending the chase period to 8 h did not change the results (data not shown). The fact that the presence of Vpu did not lead to an accelerated decay of immature BST-2 in BfA-treated CEMx174 cells indicates that Vpu does not cause an ER-associated degradation of BST-2. We therefore conclude that the rapid disappearance of immature BST-2 in infected CEMx174 cells, as shown in Fig. 3D, is due to the exit of BST-2 from the ER and subsequent carbohydrate modification and is not caused by ER-associated protein degradation as in the case of CD4.

Exogenously expressed Vpu induces ER-associated degradation of immature BST-2. Several studies reported that Vpu reduces BST-2 levels in a TrCP-dependent manner (7, 11, 26,
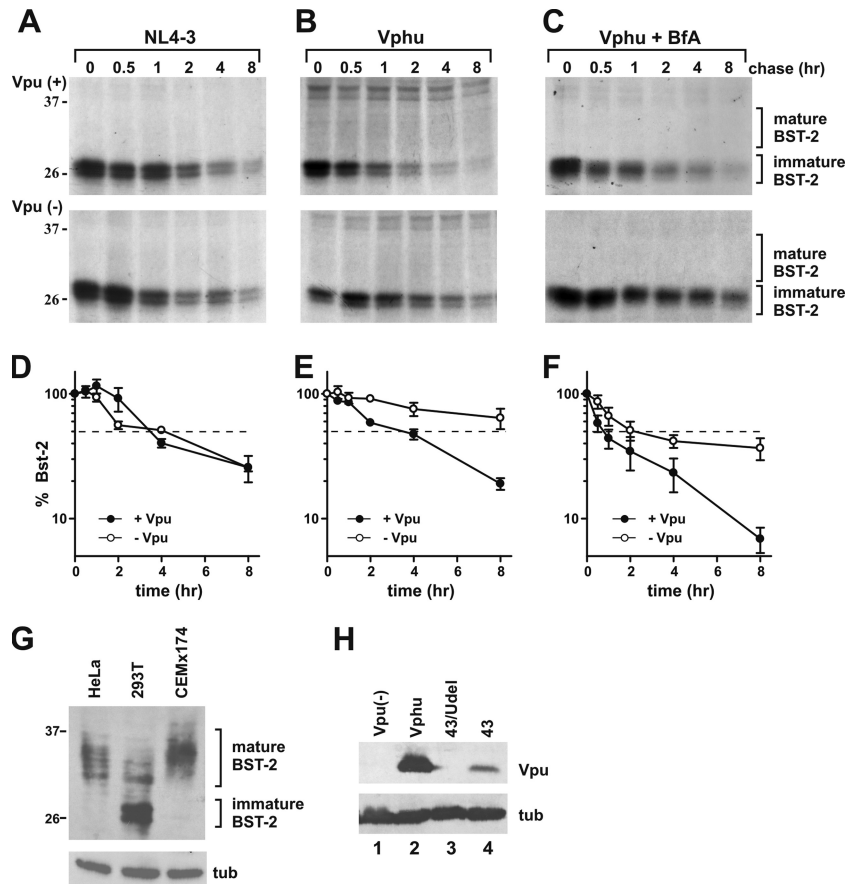
FIG. 5. Transfected BST-2 in 293T cells is destabilized by VphU but not Vpu. (A) 293T cells were transfected with 1 μg of pCDNA-BST-2 with 4 μg of either wt NL4-3 virus (closed circles) or NL4-3/Udel virus (open circles). (B) 293T cells were transfected with 1 μg of pcDNA-BST2 with (closed circles) or without (open circles) 2 μg pcDNA-VphU. Total DNA was adjusted to 5 μg with empty vector DNA. (C) 293T cells were transfected as described above (B), with the addition of brefeldin A during the pulse and chase at 5 μg/ml. In all experiments, 24 h after transfection cells were pulse-labeled for 1 h at 37°C by the addition of ^{35}S-labeled amino acids and chased for the indicated time intervals in complete medium. BST-2 was immunoprecipitated with specific antibodies. Representative results are shown. The position of molecular weight standards is shown on the left. (D to F) The percentage of immature BST-2 remaining at each time point was calculated relative to the signal at time zero. Plotted data are derived from three independent experiments. Error bars represent standard errors of the means. (G) Cell lysates from 293T cells transfected with 1 μg of BST-2 as well as HeLa and CEMx174 cell extracts were separated by SDS-PAGE and subjected to immunoblot analysis with antibodies to BST-2 and tubulin (tub). The position of molecular weight standards is shown on the left. (H) 293T cells were transfected with 1 μg of pcDNA-BST2 in the absence of Vpu (lane 1) or together with 2 μg of pcDNA-VphU (lane 2), 4 μg of pNL4-3/Udel (lane 3), or 4 μg of pNL4-3 DNA (lane 4). Total DNA was adjusted to 5 μg with empty vector DNA. Lysates were separated by SDS-PAGE and subjected to immunoblot analysis with antibodies to Vpu, or tubulin (tub).

29). Whether this involves the TrCP-dependent proteasomal degradation of newly synthesized protein is still under debate. Two studies found that treatment with proteasome inhibitors inhibited BST-2 degradation by Vpu (11, 26), while others failed to observe a stabilizing effect of proteasome inhibitors (7, 29). Our next goal, therefore, was to test if the observed effects of Vpu on the stability of endogenous BST-2 in HeLa cells and CEMx174 cells were also true for transiently expressed BST-2 in 293T cells. For that purpose, 293T cells were transfected with a BST-2-encoding vector together with either pNL4-3 or pNL4-3/Udel (Fig. 5A) or the codon-optimized Vpu expression vector pcDNA-Vphu (Fig. 5B and C). A pulse-chase analysis was performed as described in the legend of Fig. 2B. As observed for HeLa and CEMx174 cells, the primary product of BST-2 expression was the 29-kDa immature form that gradually disappeared during the subsequent chase. In

contrast to HeLa and CEMx174 cells, we failed to immuno-precipitate significant amounts of mature BST-2. The reason for that is not clear. However, the rate of *de novo* BST-2 synthesis in transfected 293T cells is much higher than the rate of synthesis of endogenous BST-2 in HeLa or CEMx174 cells. This could create a bottleneck effect at the exit of BST-2 from the ER and result in the accumulation of immature ER-associated BST-2 (3). Indeed, immunoblot analyses verified the predominance of immature BST-2 in transiently transfected 293T cells relative to endogenous BST-2 in HeLa or CEMx174 cells (Fig. 5G). Because of that, we focused on the quantitation of immature BST-2 and refrained from quantifying mature BST-2 in this experiment. Consistent with our results with HeLa and CEMx174 cells, Vpu expressed from the full-length viral genome had no effect on the stability of immature BST-2 in transiently transfected 293T cells (Fig. 5A and D). In con-

trast, Vpu expressed from the codon-optimized vector accelerated the decay of immature BST-2 (Fig. 5B and E, closed circles) compared to the Vpu-negative control (Fig. 5B and E, open circles). Surprisingly, BfA treatment did not stabilize immature BST-2 (Fig. 5C and F). This finding suggests that the disappearance of immature BST-2 in this case is most likely due to ER-associated proteasomal degradation and not due to the conversion of immature BST-2 to mature BST-2. The differential effect of virus-encoded Vpu versus Vphu expressed from a codon-optimized vector could be explained by the higher levels of the Vphu protein than virus-encoded Vpu from transfected cells (Fig. 5H).

DISCUSSION

The recent discovery that the interferon-inducible host factor BST-2/tetherin inhibits HIV virus release, which can be antagonized by Vpu (33, 42), has reenergized the Vpu field and stimulated investigations of the underlying molecular mechanisms. While the intriguing structural properties of BST-2 quickly led to a model in which BST-2 functions as a molecular tether (hence the name tetherin [33]), the actual experimental evidence for the involvement of a tethering mechanism in the restriction of virus release remains indirect. Also, it is unclear exactly how Vpu antagonizes the antiviral effect of BST-2. We previously reported that in the course of a productive infection in T cell lines, efficient virus release did not correlate with a cell surface down-modulation of BST-2 (30). In single-cycle infections or transient-transfection studies, however, Vpu is generally found to downregulate BST-2 from the cell surface, especially when Vpu is expressed at high levels (Fig. 1A) (7, 17, 30, 42). Even so, the surface downregulation of BST-2 is never complete (Fig. 1A and B) (30), and, while consistent with a tethering model, it remains to be determined whether the Vpu-induced reduction in the level of cell surface BST-2 is a prerequisite for enhanced virus release or a downstream effect of Vpu function.

Our data confirm previous studies indicating that Vpu does not accelerate the rate of BST-2 internalization from the cell surface (8, 29). In fact, it appears from our data, which are derived from five independent experiments, that Vpu slows down BST-2 internalization. This effect of Vpu is unexplained and seems paradoxical in light of the fact that the net effect of Vpu is the reduced cell surface expression level of BST-2. However, a similar trend, albeit not quite as pronounced, was observed in two previous studies (8, 29). In addition, the fact that internalized BST-2 quickly establishes a steady-state equilibrium at ~60 to 80% of the starting level (Fig. 1B) suggests that Vpu does not inhibit the recycling of internalized BST-2 to a significant extent, as suggested previously (29). On the basis of these observations we propose that Vpu blocks the resupply of BST-2 from the pool of *de novo*-synthesized protein (Fig. 6). The uncoupling of BST-2 cycling at the cell surface from the transport of *de novo*-synthesized BST-2 could explain why the surface down-modulation of BST-2 by Vpu is incomplete. Thus, the cell surface down-modulation of BST-2 in Vpu-expressing cells is presumably due to an effect on the resupply of BST-2 from within the cell rather than a direct effect of Vpu on cell surface BST-2 (Fig. 6).

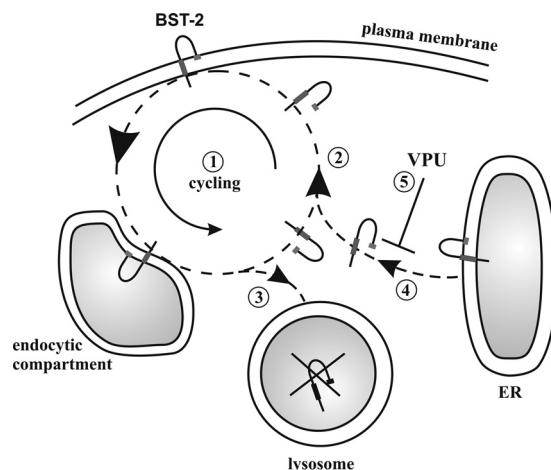Several previous studies reported that Vpu reduces BST-2

FIG. 6. Model for the interference of Vpu with cell surface expression of BST-2. BST-2 expressed at the cell surface is not static but cycles between the endocytic compartment and the cell surface (1). The majority of internalized BST-2 (as indicated by the size of the arrowhead) is recycled to the cell surface (2). A small fraction of internalized BST-2 molecules is not recycled to the surface but remains inside the cell and is targeted for degradation in the lysosomal compartment (3). The BST-2 population at the cell surface is maintained at constant levels by replacing the nonrecycled portion of BST-2 with *de novo*-synthesized protein from the endoplasmic reticulum (ER) (4). The interference of Vpu with the resupply (5) results in the gradual depletion of cell surface BST-2.

levels in a TrCP-dependent manner (7, 8, 11, 26, 29). Those studies either analyzed the entire population of immature and mature BST-2 (8) or took into account only the dominant immature form (7, 11). Using similar analytical approaches, we arrived at similar conclusions by demonstrating that (i) virus-encoded Vpu increases the rate of turnover of total BST-2 in infected HeLa (Fig. 2C) and CEMx174 (Fig. 3C) cells and (ii) the high-level expression of Vpu accelerates the degradation of newly synthesized immature BST-2 through an ER-associated pathway (Fig. 5B). Importantly, our study revealed an interesting and important difference between the effect of virus-encoded and exogenously expressed Vpu on the stability of BST-2. Our data clearly show that virus-encoded Vpu does not cause the degradation of immature BST-2 in HeLa (Fig. 2D), CEMx174 (Fig. 3D), or 293T (Fig. 5B) cells. As such, the results from our current study are consistent with our previous work on the role of Vpu in regulating virus release (41) and demonstrate that the Vpu-mediated degradation of CD4 and down-modulation of BST-2 are mechanistically distinct. Previous studies analyzing the mechanism of the Vpu-mediated degradation of CD4 found that BfA treatment greatly accelerated the turnover of CD4 because CD4 was unable to exit the ER and thus remained fully accessible to Vpu (43). In contrast, the treatment of HIV-infected CEMx174 cells with BfA did not increase BST-2 turnover but, in fact, stabilized BST-2 (Fig. 4C), further supporting our conclusion that virus-encoded Vpu does not induce an ER-associated degradation of BST-2. On the other hand, our findings that exogenously expressed Vpu was able to increase the turnover of immature BST-2 in transfected 293T cells and that this effect was not inhibited by BfA treatment (Fig. 5E and F) indicate that Vpu can indeed cause proteasomal degradation, as reported previ-

ously (11, 26). We conclude that Vpu can increase the turnover of both immature and mature BST-2 through different mechanisms. Immature BST-2 is degraded in the ER, presumably through an ER-associated pathway, as recently described (11, 26), while mature BST-2 is degraded in a post-ER compartment, presumably the lysosomal pathway, consistent with data from previous reports (7, 20, 29). It is not quite clear why virus-encoded Vpu fails to degrade immature BST-2 in virus-producing HeLa, CEMx174, and 293T cells. All Vpu proteins used in this study are based on the NL4-3 isolate, thus ruling out strain-specific variation. It is possible, however, that the observed differences between virus-encoded and autonomously expressed Vpu are caused by a simple dose-effect. The codon-optimized Vpu vector used in this study for the autonomous expression of Vpu produces about 10-times-more Vpu (per μg transfected DNA) than the full-length proviral vector (Fig. 5H) (34). It is therefore possible that the enhanced degradation of immature BST-2 shown in Fig. 5E is caused by the high-level expression of Vpu. Also, the fact that BfA treatment did not stabilize immature BST-2 in transfected 293T cells even in the absence of Vpu indicates that a significant portion of transiently expressed immature BST-2 is not converted to mature BST-2 but is retained in the ER and ultimately degraded even without Vpu.

In conclusion, the results from our current study demonstrate that Vpu does to a limited extent increase the turnover of BST-2 both in infected as well as in transiently transfected cells. However, the effects of Vpu on BST-2 stability are relatively subtle and do not substantially affect the total amounts of cell-associated BST-2 (8, 30). This leads us to conclude that Vpu regulates virus release from a post-ER compartment, possibly the *trans*-Golgi network, as previously suggested (8), and selectively targets *de novo*-synthesized BST-2 by inhibiting its transport to the cell surface (Fig. 6). As a consequence, *de novo*-synthesized BST-2 is presumably redirected to the lysosomal compartment for degradation, leading to the net depletion of BST-2 from the cell surface.

REFERENCES

1. **Adachi, A., et al.** 1986. Production of acquired immunodeficiency syndrome-associated retrovirus in human and nonhuman cells transfected with an infectious molecular clone. J. Virol. **59:**284–291.
2. **Andrew, A., and K. Strebel.** 2010. HIV-1 Vpu targets cell surface markers CD4 and BST-2 through distinct mechanisms. Mol. Aspects Med. **31:**407–417.
3. **Andrew, A. J., E. Miyagi, S. Kao, and K. Strebel.** 2009. The formation of cysteine-linked dimers of BST-2/tetherin is important for inhibition of HIV-1 virus release but not for sensitivity to Vpu. Retrovirology **6:**80.
4. **Asaoka, K., et al.** 2005. A retrovirus restriction factor TRIM5alpha is transcriptionally regulated by interferons. Biochem. Biophys. Res. Commun. **338:**1950–1956.
5. **Bartee, E., A. McCormack, and K. Fruh.** 2006. Quantitative membrane proteomics reveals new cellular targets of viral immune modulators. PLoS Pathog. **2:**e107.
6. **Binette, J., et al.** 2007. Requirements for the selective degradation of CD4 receptor molecules by the human immunodeficiency virus type 1 Vpu protein in the endoplasmic reticulum. Retrovirology **4:**75.
7. **Douglas, J. L., et al.** 2009. Vpu directs the degradation of the human immunodeficiency virus restriction factor BST-2/tetherin via a βTrCP-dependent mechanism. J. Virol. **83:**7931–7947.
8. **Dube, M., et al.** 2010. Antagonism of tetherin restriction of HIV-1 release by Vpu involves binding and sequestration of the restriction factor in a perinuclear compartment. PLoS Pathog. **6:**e1000856.
9. **Dube, M., et al.** 2009. Suppression of tetherin-restricting activity upon human immunodeficiency virus type 1 particle release correlates with localization of Vpu in the trans-Golgi network. J. Virol. **83:**4574–4590.
10. **Fitzpatrick, K., et al.** 2010. Direct restriction of virus release and incorporation of the interferon-induced protein BST-2 into HIV-1 particles. PLoS Pathog. **6:**e1000701.
11. **Goffinet, C., et al.** 2009. HIV-1 antagonism of CD317 is species specific and involves Vpu-mediated proteasomal degradation of the restriction factor. Cell Host Microbe **5:**285–297.
12. **Goffinet, C., et al.** 2010. Antagonism of CD317 restriction of HIV-1 particle release and depletion of CD317 are separable activities of HIV-1 Vpu. J. Virol. **84:**4089–4094.
13. **Goto, T., et al.** 1994. A novel membrane antigen selectively expressed on terminally differentiated human B cells. Blood **84:**1922–1930.
14. **Gupta, R. K., et al.** 2009. Mutation of a single residue renders human tetherin resistant to HIV-1 Vpu-mediated depletion. PLoS Pathog. **5:**e1000443.
15. **Habermann, A., et al.** 2010. CD317/tetherin is enriched in the HIV-1 envelope and downregulated from the plasma membrane upon virus infection. J. Virol. **84:**4646–4658.
16. **Hammonds, J., J. J. Wang, H. Yi, and P. Spearman.** 2010. Immunoelectron microscopic evidence for tetherin/BST2 as the physical bridge between HIV-1 virions and the plasma membrane. PLoS Pathog. **6:**e1000749.
17. **Hauser, H., et al.** 2010. HIV-1 Vpu and HIV-2 Env counteract BST-2/tetherin by sequestration in a perinuclear compartment. Retrovirology **7:**51.
18. **Hinz, A., et al.** 2010. Structural basis of HIV-1 tethering to membranes by the BST-2/tetherin ectodomain. Cell Host Microbe **7:**314–323.
19. **Ishikawa, J., et al.** 1995. Molecular cloning and chromosomal mapping of a bone marrow stromal cell surface gene, BST2, that may be involved in pre-B-cell growth. Genomics **26:**527–534.
20. **Iwabu, Y., et al.** 2009. HIV-1 accessory protein Vpu internalizes cell-surface BST-2/tetherin through transmembrane interactions leading to lysosomes. J. Biol. Chem. **284:**35060–35072.
21. **Klimkait, T., K. Strebel, M. D. Hoggan, M. A. Martin, and J. M. Orenstein.** 1990. The human immunodeficiency virus type 1-specific protein Vpu is required for efficient virus maturation and release. J. Virol. **64:**621–629.
22. **Kupzig, S., et al.** 2003. Bst-2/HM1.24 is a raft-associated apical membrane protein with an unusual topology. Traffic **4:**694–709.
23. **Le Tortorec, A., and S. J. Neil.** 2009. Antagonism to and intracellular sequestration of human tetherin by the human immunodeficiency virus type 2 envelope glycoprotein. J. Virol. **83:**11966–11978.
24. **Lippincott-Schwartz, J., L. C. Yuan, J. S. Bonifacino, and R. D. Klausner.** 1989. Rapid redistribution of Golgi proteins into the ER in cells treated with brefeldin A: evidence for membrane cycling from Golgi to ER. Cell **56:**801–813.
25. **Magadan, J. G., et al.** 2010. Multilayered mechanism of CD4 downregulation by HIV-1 Vpu involving distinct ER retention and ERAD targeting steps. PLoS Pathog. **6:**e1000869.
26. **Mangeat, B., et al.** 2009. HIV-1 Vpu neutralizes the antiviral factor tetherin/BST-2 by binding it and directing its beta-TrCP2-dependent degradation. PLoS Pathog. **5:**e1000574.
27. **Masuyama, N., et al.** 2009. HM1.24 is internalized from lipid rafts by clathrin-mediated endocytosis through interaction with alpha-adaptin. J. Biol. Chem. **284:**15927–15941.
28. **McNatt, M. W., et al.** 2009. Species-specific activity of HIV-1 Vpu and positive selection of tetherin transmembrane domain variants. PLoS Pathog. **5:**e1000300.
29. **Mitchell, R. S., et al.** 2009. Vpu antagonizes BST-2-mediated restriction of HIV-1 release via beta-TrCP and endo-lysosomal trafficking. PLoS Pathog. **5:**e1000450.
30. **Miyagi, E., A. J. Andrew, S. Kao, and K. Strebel.** 2009. Vpu enhances HIV-1 virus release in the absence of Bst-2 cell surface down-modulation and intracellular depletion. Proc. Natl. Acad. Sci. U. S. A. **106:**2868–2873.
31. **Neil, S. J., S. W. Eastman, N. Jouvenet, and P. D. Bieniasz.** 2006. HIV-1 Vpu promotes release and prevents endocytosis of nascent retrovirus particles from the plasma membrane. PLoS Pathog. **2:**e39.
32. **Neil, S. J., V. Sandrin, W. I. Sundquist, and P. D. Bieniasz.** 2007. An interferon-alpha-induced tethering mechanism inhibits HIV-1 and Ebola virus particle release but is counteracted by the HIV-1 Vpu protein. Cell Host Microbe **2:**193–203.
33. **Neil, S. J., T. Zang, and P. D. Bieniasz.** 2008. Tetherin inhibits retrovirus release and is antagonized by HIV-1 Vpu. Nature **451:**425–430.
34. **Nguyen, K. L., et al.** 2004. Codon optimization of the HIV-1 vpu and vif genes stabilizes their mRNA and allows for highly efficient Rev-independent expression. Virology **319:**163–175.
35. **Ohtomo, T., et al.** 1999. Molecular cloning and characterization of a surface antigen preferentially overexpressed on multiple myeloma cells. Biochem. Biophys. Res. Commun. **258:**583–591.

36. **Perez-Caballero, D., et al.** 2009. Tetherin inhibits HIV-1 release by directly tethering virions to cells. Cell **139:**499–511.

37. **Rollason, R., V. Korolchuk, C. Hamilton, P. Schu, and G. Banting.** 2007. Clathrin-mediated endocytosis of a lipid-raft-associated protein is mediated through a dual tyrosine motif. J. Cell Sci. **120:**3850–3858.

38. **Rong, L., et al.** 2009. The transmembrane domain of BST-2 determines its sensitivity to down-modulation by HIV-1 Vpu. J. Virol. **83:**7536–7546.

39. **Rose, K. M., M. Marin, S. L. Kozak, and D. Kabat.** 2004. Transcriptional regulation of APOBEC3G, a cytidine deaminase that hypermutates human immunodeficiency virus. J. Biol. Chem. **279:**41744–41749.

40. **Schubert, H. L., et al.** 2010. Structural and functional studies on the extracellular domain of BST2/tetherin in reduced and oxidized conformations. Proc. Natl. Acad. Sci. U. S. A. **107:**17951–17956.

41. **Schubert, U., et al.** 1996. The two biological activities of human immunode-ficiency virus type 1 Vpu protein involve two separable structural domains. J. Virol. **70:**809–819.

42. **Van Damme, N., et al.** 2008. The interferon-induced protein BST-2 restricts HIV-1 release and is downregulated from the cell surface by the viral Vpu protein. Cell Host Microbe **3:**245–252.

43. **Willey, R. L., F. Maldarelli, M. A. Martin, and K. Strebel.** 1992. Human immunodeficiency virus type 1 Vpu protein induces rapid degradation of CD4. J. Virol. **66:**7193–7200.

44. **Willey, R. L., et al.** 1988. In vitro mutagenesis identifies a region within the envelope gene of the human immunodeficiency virus that is critical for infectivity. J. Virol. **62:**139–147.

45. **Yang, H., et al.** 2010. Structural insight into the mechanisms of enveloped virus tethering by tetherin. Proc. Natl. Acad. Sci. U. S. A. **107:**18428–18432.